

Probability distribution functions in turbulent convection

S. Balachandar

Department of Theoretical and Applied Mechanics, University of Illinois, Urbana, Illinois 61801

L. Sirovich

Center for Fluid Mechanics, Brown University, Providence, Rhode Island 02912

(Received 17 August 1990; accepted 22 January 1991)

Results of an extensive investigation of probability distribution functions (pdf's) for Rayleigh-Bénard convection, in the hard turbulence regime, are presented. It is seen that the pdf's exhibit a high degree of internal universality. In certain cases this universality is established within two Kolmogorov scales of a boundary. A discussion of the factors leading to universality is presented.

I. INTRODUCTION

Probability distribution functions (pdf's) long have been of importance in discussing turbulent flows (see Pope¹ for a comprehensive review to 1985). They serve as a valuable tool in presenting data and give valuable insights into range of behavior. Recent work²⁻⁵ has placed a new emphasis on their study in turbulent flows. Direct numerical simulations⁶⁻⁹ and improved experimental techniques¹⁰⁻¹² have permitted more detailed pdf's, and allow us to go well beyond such low-order moments as variances σ , skewness s , and flatness f , common in the statistical description of turbulent flows. Part of the recent interest in pdf's is due to the experiments of the Chicago group,¹⁰⁻¹² and in particular to the *exponential* tails they observed for the pdf's of temperature fluctuations. The wide *tails* of such pdf's *underline the essential role that intermittency* plays in turbulence phenomena. However, earlier investigations also led to such exponential distributions.¹³⁻¹⁵

On the theoretical side, Sinai and Yakhot² considered the pdf of a passive scalar and made remarkable progress in describing the limiting distribution function. Subsequent to this, Yakhot and co-workers^{3,16} extended this approach and presented arguments leading to exponential pdf's for temperature fluctuations and vorticity. Kraichnan has also made a notable extension to this approach.⁵ More recently Kraichnan^{17,18} has produced a relatively simple *closure* model based on the mechanisms at work in fluid flow that lead to wide skirted pdf's.

In this paper we present the results of an extensive study of pdf's as generated in a computational investigation of the Rayleigh-Bénard (RB) convection problem. The present results are based on a substantially longer simulation than was considered in our earlier publications.^{6,7} For purposes of comparison we estimate the turnover time by

$$\tau = H/q_{\text{rms}}, \quad (1)$$

where H is the height of the computational cell and q_{rms} represents the rms speed. In such terms our earlier work was based on 4.65 turnover times while the present study is based on 41.7 turnover times.

The specification of the problem as well as the details of the calculation appear in our earlier work.^{6,7} In brief, we simulate turbulent thermal convection as described by the Boussinesq equations.¹⁹ The vertical coordinate is denoted by z and the horizontal by x and y . The horizontal planform is a square and the aspect ratio (width to height) is $2\sqrt{2}$. The

Rayleigh number is 0.98×10^4 times the critical Rayleigh number of $27\pi^4/4$, which places the simulation in the range of hard turbulence in the terminology of the Chicago group.¹⁰⁻¹² The velocity satisfies slip boundary conditions on the impermeable horizontal boundaries and temperature is specified on these walls. Periodic boundary conditions are imposed in both horizontal directions.

The calculation uses 96 equal grid spacing in the vertical direction, with a like number in each of the horizontal directions. Since the Nusselt number, Nu , is roughly 23 for this calculation and since

$$Nu \approx H/2\delta, \quad (2)$$

where δ is the thickness of the thermal sublayer, two grid spacings lie in the sublayer. (The sublayer thickness is also a measure of the Kolmogorov scale.) These few facts are useful in interpreting the material that follows since various quantities will be specified by their vertical grid spacing locations.

As will be seen the pdf's exhibit a remarkable degree of universality. By universality we mean the unanticipated lack of dependence on strongly inhomogeneous directions. As discussed in Sec. VI the same universality is expected to extend to other convection problems if the pdf's are suitably normalized.

II. PRELIMINARY CONSIDERATIONS

In general if α represents a dependent variable, then we will denote by

$$P_\alpha = P\left(\frac{\alpha - \bar{\alpha}}{[(\alpha - \bar{\alpha})^2]^{1/2}}\right) = P(\hat{\alpha}), \quad (3)$$

the pdf which will be plotted in our figures. The bar signifies that the quantity has been averaged in time as well as over a horizontal plane. As previously reported for Bénard convection^{6,7} temperature pdf's vary considerably in the vertical direction. Figure 1 shows the pdf of temperature fluctuation T' at six different elevations. (See the cited reference for more details of the calculation and notation.) The temperature pdf at the edge of the thermal sublayer ($z = \frac{1}{6}$) though not symmetric, has skewness close to zero. Above the bottom sublayer ($z = \frac{1}{6}, \frac{1}{3},$ and $\frac{1}{2}$) the pdf's exhibit a peak corresponding to a small negative value and a long positive tail, resulting in significant positive skewness. This indicates the existence of hot thermal plumes near the bottom boundary

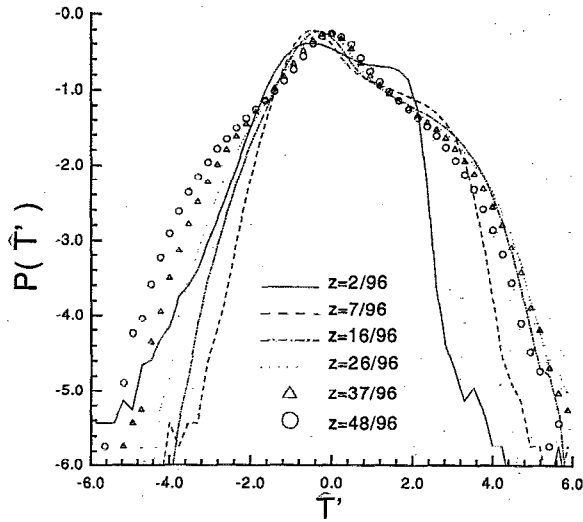


FIG. 1. Probability distribution function of normalized temperature fluctuation $\hat{T}' = (T' - \overline{T'}) / \sqrt{(T' - \overline{T'})^2}$ at six different heights from the bottom boundary. $z = \frac{2}{96}$ is at the edge of the bottom thermal sublayer, $z = \frac{7}{96}$ is in the region of hot thermal plumes, and $z = \frac{16}{96}$ is roughly at the edge of the plume region. $z = \frac{26}{96}$, $\frac{37}{96}$, and $\frac{48}{96}$ are in the turbulent core. The results corresponding to the top half can be extended from the bottom half based on symmetry conditions.

and at the midplane the pdf is symmetric. Figure 2 shows the comparable pdf's for the horizontal velocity u and vertical velocity w . The parabolic shape of the u pdf in this log-linear plot indicates the Gaussian nature of the distribution. At the midplane the pdf of w exhibits a similar Gaussian nature, whereas below the midplane the pdf of w is positively skewed similar to the temperature pdf's but to a much lesser extent.

In our earlier papers we confirmed the existence of an exponential range to the pdf for fluctuations in temperature in the midplane as first exhibited by the Chicago group. This result was based on less than three log units range in the pdf. With the increased database, we now have reliable data for a range of almost six log units as exhibited in Fig. 1. While the pdf in the midplane is still fit by an exponential over the first two to three log units the overall picture is quite different. The reason for the sharp down turn in the tails of the pdf is easy to understand. Since the temperature fluctuations are bounded below and above by the wall temperatures, the skirts of the pdf $P(\hat{T}')$ must terminate at finite values. This tendency is clearly exhibited by the midplane pdf shown in Fig. 1. A brief summary describing the shape of the $P(\hat{T}')$ at the midplane is (i) first, analytical considerations dictate that the pdf must be rounded at the center; (ii) second, this is followed by wide skirts, fit by an exponential, and which indicate relatively large fluctuations; (iii) finally, limited temperature fluctuations dictated by the wall temperatures force a rapid falloff of the skirts.

In viewing the preceding pdf's and those to be presented later it is important to keep in mind the symmetries of the problem. This is especially true of the pdf's measured in the midplane of the cell $z = \frac{48}{96}$, since some pdf's become symmetric only in the midplane. As has been shown, the problem under discussion has a 16-fold symmetry group.²⁰ We have not made use of this to extend the database (and thus shar-

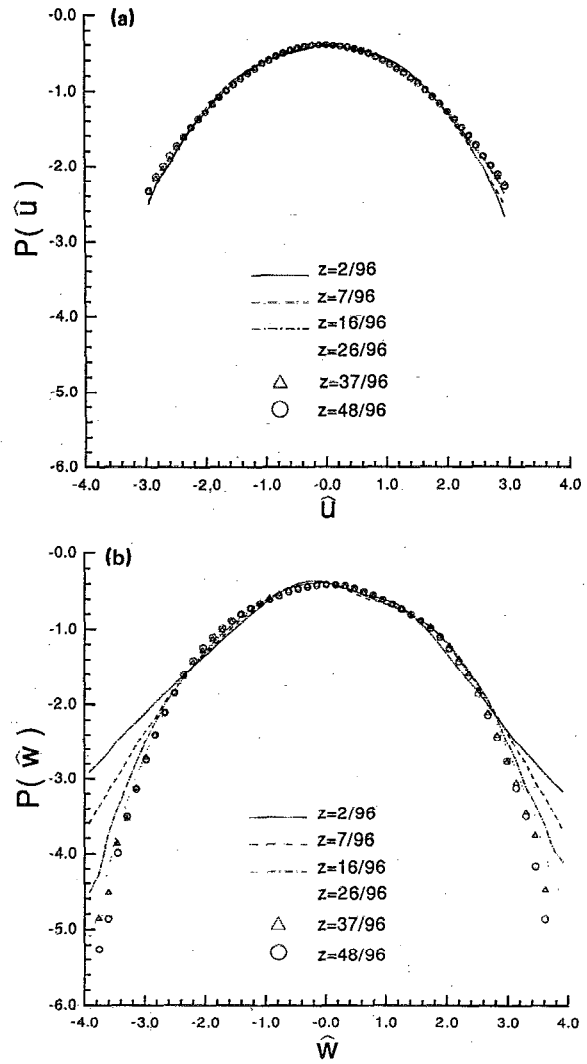


FIG. 2. (a) Same as Fig. 1 but for \hat{u} . (b) Same as Fig. 1 but for \hat{w} .

pen the pdf curves) but instead have verified these symmetries to support the correctness of data. [For example, $P(\hat{v})$, not shown, is virtually identical to $P(\hat{u})$, Fig. 2(a).] In considering the pdf's it is useful to split these into two classes. Those that must have symmetric distributions as a result of an inherent symmetry and those for which there is no *a priori* symmetry requirement. In general, if we consider a pdf $P(\hat{\alpha})$, and if there exists an admissible transformation of the group G such that

$$G\alpha = -\alpha, \quad (4)$$

then this implies that

$$P(\hat{\alpha}) = P(-\hat{\alpha}). \quad (5)$$

Consider, for example, the horizontal velocity u . Under reflection in the plane $x = 0$, $u \rightarrow -u$, and hence $P(\hat{u})$ is symmetric for all z values. This is clearly indicated in Fig. 2(a). Alternately, both the vertical velocity w and the temperature fluctuation T' go into their negatives under reflection in the midplane, but not elsewhere. Thus their midplane pdf's should be symmetric and as seen in Figs. 1 and 2(b), this is the case. However no group operation produces (4) at

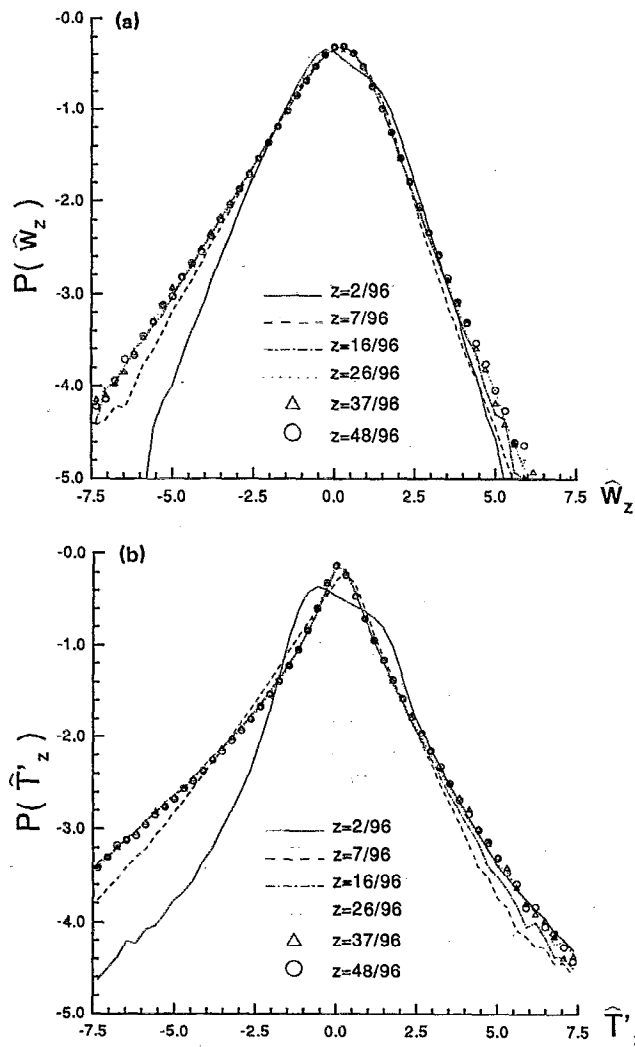


FIG. 3. (a) Same as Fig. 1 but for \hat{w}_z . (b) Same as Fig. 1 but for \hat{T}'_z .

other z elevations and there is no reason for these pdf's to be symmetric for other values of z . This is borne out by Figs. 1 and 2(b).

We can carry this line of reasoning somewhat further and consider w_z and T'_z , neither of which have a group operation leading to (4). Figures 3(a) and 3(b) show the pdf's for each of these quantities. As can be seen the corresponding pdf's show no symmetry at any z value. This can be given a physical interpretation. Away from the two thin sublayers near the top and the bottom boundaries the pdf's are negatively skewed. To see this consider a parcel of fluid located at some height z' traveling up. Since the vertical velocity and temperature fluctuations are well correlated, the probability that this parcel of fluid has positive temperature fluctuation is high. After a small time interval the fluid parcel will be at a higher elevation $z' + \delta z'$ surrounded by relatively colder fluid. Therefore the probability that this parcel will accelerate up ($w_z > 0$) and contribute larger temperature fluctuation ($T'_z > 0$) is high. Similarly if we consider a parcel of fluid with negative temperature fluctuation moving down, the probability that the parcel will accelerate down ($w_z > 0$) with larger temperature fluctuation ($T'_z > 0$) is large.

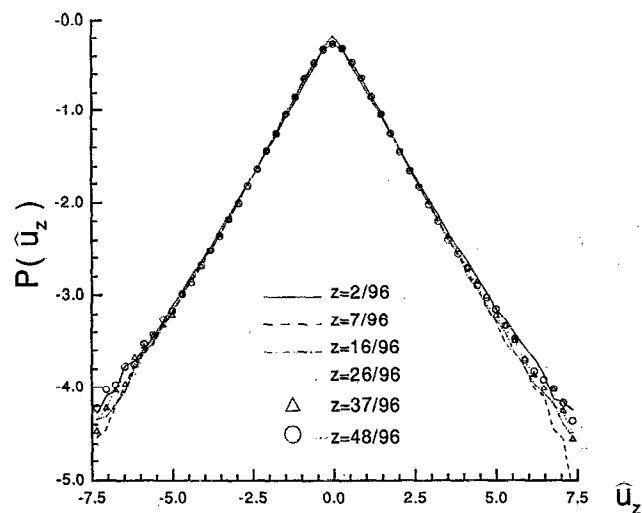


FIG. 4. Same as Fig. 1 but for \hat{u}_z .

Therefore both w_z and T'_z show a peak in their probability distribution at a (small) positive value and this peak is compensated by a less steep negative tail, in order to yield zero mean values. For the $P(\hat{w}_z)$ this negative tail can be associated with the less probable event of rapid deceleration of both the up moving cold parcel of fluid and the down moving warm parcel of fluid. In other words, mild acceleration up or down is more probable than mild deceleration, but rapid deceleration (up or down) is more probable than rapid acceleration. Similar interpretations can be given for the gradient of the temperature fluctuations as well, and in general the pdf of a quantity provides us with a view of its range of behavior.

For comparison with the pdf's of Fig. 3, we consider u_z which has a symmetry leading to (5) for all z . The corresponding pdf is shown in Fig. 4. This clearly indicates the symmetry but in addition shows a remarkable degree of universality in the z direction. Such universality will be encountered for the majority of the pdf's which will be presented below. Further discussion of this unexpected property will be presented in the following sections.

III. PROBABILITY DISTRIBUTION FUNCTIONS

As already seen in Fig. 4 the pdf of u_z (or equivalently v_z) exhibits a surprising universality across the convective cell. To explore this property further we present, in Fig. 5, the components of vorticity. The pdf's for the horizontal components Ω_1 and Ω_2 are virtually identical, only Ω_1 is shown, and in addition exhibit a high degree of universality. Vertical vorticity Ω_3 , on the other hand, shows a significant departure from universality. All vorticity components lead to pdf's that satisfy (4), either through reflection in a plane of constant x or y .

Given that mechanisms are at work that force universality, we should expect in general that boundaries will produce significant departures from universality. To contrast the results of the pdf's for the horizontal and vertical components

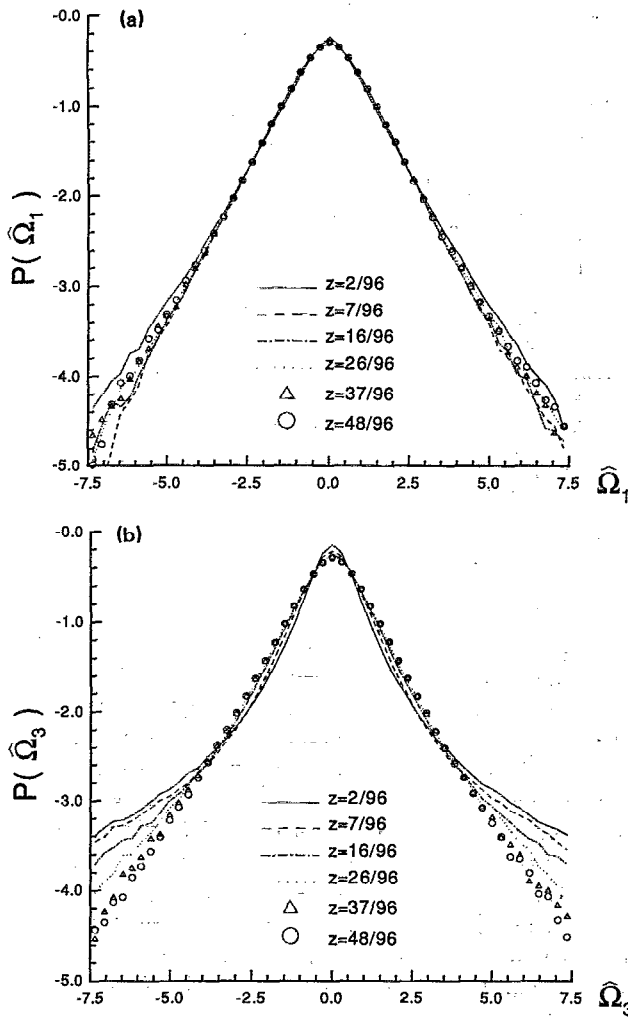


FIG. 5. (a) Same as Fig. 1 but for $\hat{\Omega}_1$. (b) Same as Fig. 1 but for $\hat{\Omega}_3$.

we recall that

$$\Omega_1 = \left(\frac{\partial w}{\partial y} - \frac{\partial v}{\partial z} \right), \quad (6)$$

$$\Omega_3 = \left(\frac{\partial v}{\partial x} - \frac{\partial u}{\partial y} \right). \quad (7)$$

It follows from the boundary conditions for this particular RB convection problem¹⁹ that $\Omega_1 \equiv 0$ (and $\Omega_2 \equiv 0$) at a wall, while Ω_3 is unrestricted at a wall. As a general principle one should expect that all permissible fluctuations will appear in the corresponding pdf with an appropriate probability. This can be seen in Fig. 5. Thus Ω_3 , which is unrestricted at the boundary has a wide skirt at $z = \frac{z}{96}$, while Ω_1 which is restricted at the wall can only develop a slight skirt in the neighborhood of the wall $z = \frac{z}{96}$. As a result universality does not appear in $P(\hat{\Omega}_3)$ until we approach the central region, where the pdf is fit by the universal curve. On the other hand universality is quickly achieved for $P(\hat{\Omega}_1)$ and $P(\hat{\Omega}_2)$. It should be noted that in the central region the pdf of all three components of vorticity are well fit by the same exponential over at least three decades. Further the pdf's of those velocity derivatives that constitute the three components of vorticity (u_y, u_z, v_x, v_z, w_x , and w_y), coincide with the above expo-

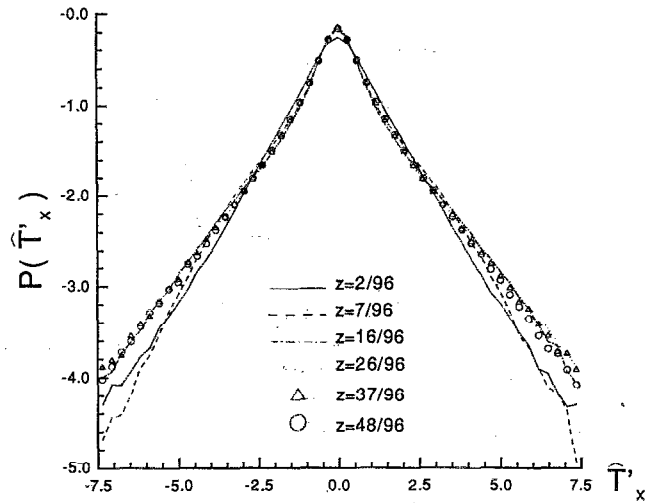


FIG. 6. Same as Fig. 2 but for \hat{T}'_x .

nential distribution (for example, see Fig. 4).

We have already seen in Figs. 1 and 3 examples of pdf's that show a strong departure from universality. For each of these pdf's the quantity in question does not satisfy the symmetry property (4) except possibly at the center plane. Both u_x and v_y are linked to w_z through the continuity equation. Since neither of these quantities have a transformation leading to (5), their pdf's lack universality. The pdf's for u_x and v_y closely resemble those shown in Fig. 3(a) and are not presented here. (Only the pdf of w_z at $z = \frac{z}{96}$ is significantly different.) [Although u_x and v_y are identically distributed, they are correlated, since the convolution of $P(\hat{u}_x)$ with itself does not produce $P(\hat{w}_z)$.]

The pdf's for w_x , with high accuracy lie on those of Ω_1 , Fig. 5(a). By contrast with the pdf in w , Fig. 2(b), this is universal except very near the wall. Thus taking a derivative of w , which then leads to a symmetrizing transformation (4), produces a quick transition to universality. In addition, the value of w_x is pinned to be equal to zero at both the top and bottom boundaries. This transition to universality is less true for T'_x , the pdf of which is shown in Fig. 6. We recall, however, that the pdf of T' itself, Fig. 1, is far less universal and significantly more skewed than the pdf of w , Fig. 2(b).

In general it can be observed that temperature statistics obey universality over a narrower region near the midplane than their velocity counterpart. This reluctance toward universality can be, at least partially, attributed to the highly intermittent nature of temperature and its derivative signals. For example, at the midplane while the pdf's of u and w are Gaussian the pdf of T' is exponential and while the pdf of vorticity is exponential the pdf of T'_x is flatter than an exponential.

IV. PDF'S FOR HIGHER DERIVATIVES

By taking derivatives of flow variables we emphasize the smaller scales. It is a widely held view that small scales forget their large scales origins. This concept lies at the heart of the $-\frac{3}{2}$ Kolmogorov range²¹ and of the exponential dissipative range.²² Both these energy ranges represent universal be-

havior of turbulent flows. Thus, as derivatives of flow quantities are increased their pdf's depend more heavily on the higher wave numbers and a tendency toward universality should be expected. Probability distribution functions of derivatives say something about distributions in small eddies:

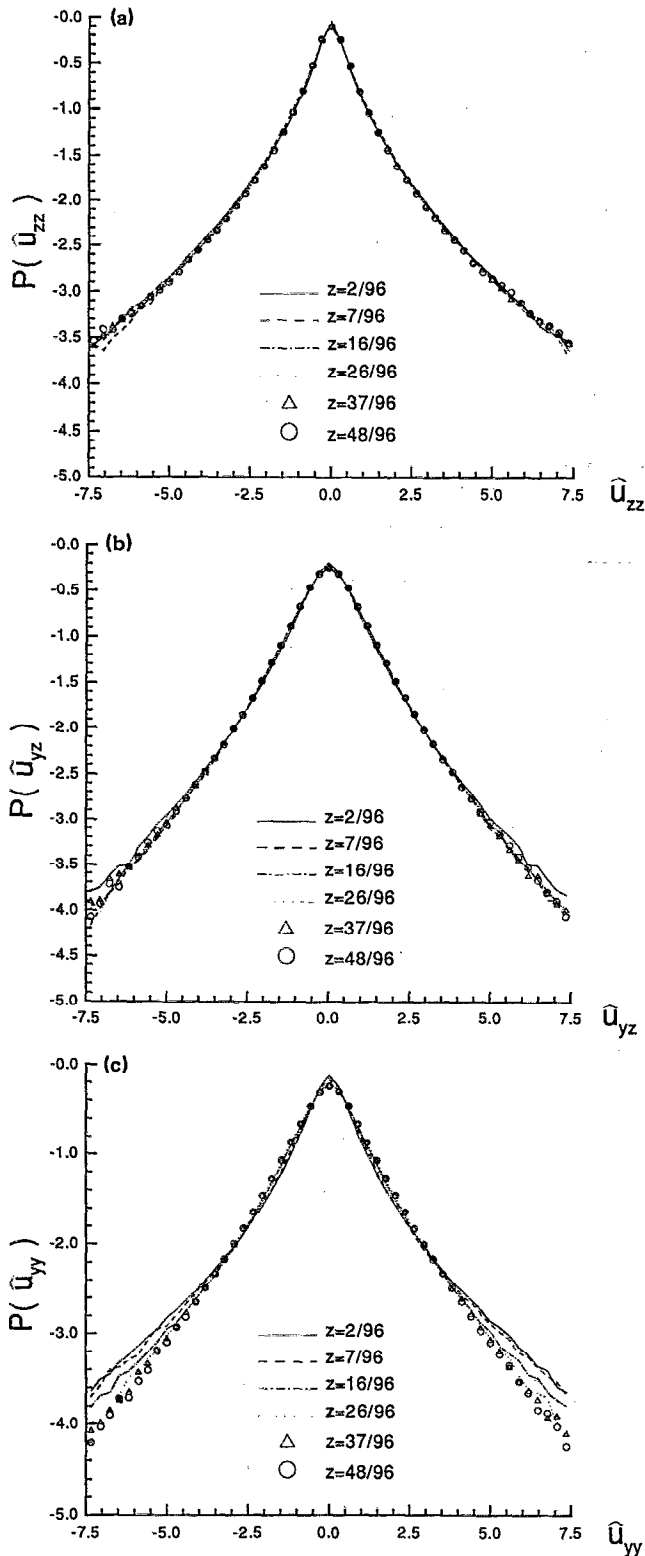


FIG. 7. (a) Same as Fig. 1 but for \hat{u}_{zz} . (b) Same as Fig. 1 but for \hat{u}_{yz} . (c) Same as Fig. 1 but for \hat{u}_{yy} .

the higher the derivative the smaller the dominant eddy. What must be regarded as remarkable is that even pdf's of first derivatives show universality. It would appear that more than the above-mentioned universal ranges are at work in producing universality, and very probably that dynamics is important in establishing at least some of the universal features.

In this section we consider the effect of taking additional derivatives of flow quantities on the corresponding pdf's. In Figs. 7-9 we exhibit a selection of second derivatives of flow quantities. These show a higher degree of universality than their first derivative counterparts. Before commenting on these in detail, we observe that all the pdf's shown in these figures exhibit a flared out skirt and are no longer fit by a simple exponential. To account for this effect, we refer to an argument given sometime ago by Kraichnan²³ that demonstrates that greater intermittency is to be expected as the wave number is increased. His argument is largely independent of Reynolds number. Thus in viewing pdf's of higher derivatives of flow quantities we should expect increasing intermittency and hence wider flaring skirts in the pdf's.

In Figs. 7(a) and 7(b) we show the pdf's for u_{zz} and u_{yz} ,

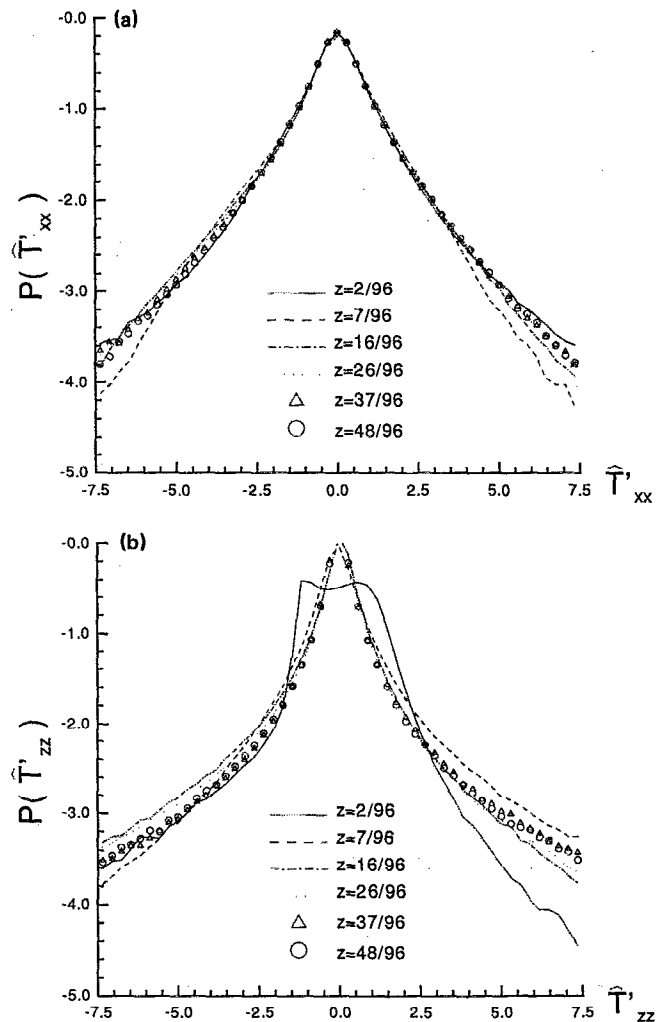


FIG. 8. (a) Same as Fig. 1 but for \hat{T}'_{xx} . (b) Same as Fig. 1 but for \hat{T}'_{zz} .

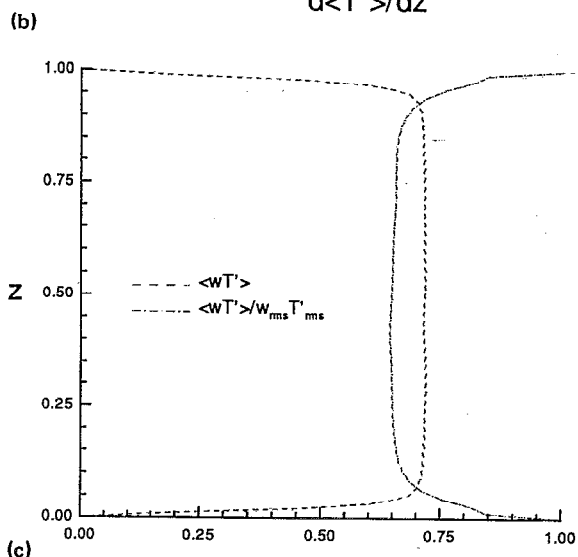
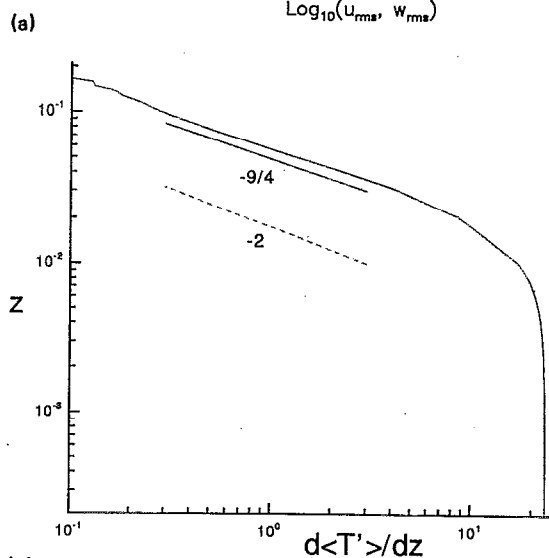
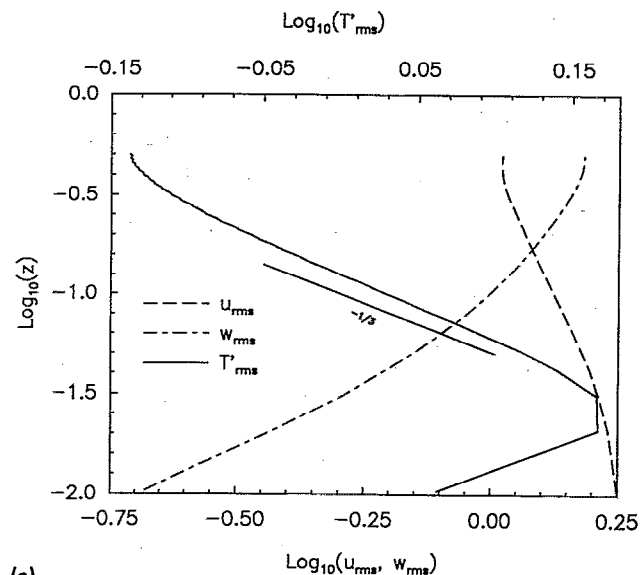


FIG. 9. (a) A log-log plot of rms temperature, vertical velocity, and horizontal velocity fluctuations against z . A straight line with $-\frac{1}{3}$ slope is compared to T'_{rms} . (b) A log-log plot of $d\langle T' \rangle/dz$ against z . For comparison -2 and $-\frac{9}{4}$ slopes are also shown in this figure. (c) Variation in wT' correlation and the covariance $\langle wT' \rangle/w'_{rms} T'_{rms}$ with respect to the vertical distance.

both of which exhibit strong universality. On the other hand pdf's for u_{yy} shown in Fig. 7(c) exhibit some departure from universality. Here u_{yz} is identically equal to zero at both boundaries, due to the stress-free boundary condition, therefore a strong tendency toward universality can be expected. Though the boundary condition is not prescribed, variations in u_{zz} will be small since it is the vertical gradient of u_z that is identically equal to zero at boundaries. As seen earlier, functions that are fixed at the boundaries quickly attain universality and within the universal regime the vertical gradients as well as the horizontal gradients can be expected to be bounded and exhibit strong universality. On the contrary, u_{yy} is neither fixed at the boundary nor does it represent the derivative of a quantity that exhibits universality.

We do not show the three pdf's corresponding to w_{xx} , w_{zz} , and w_{xz} since they virtually lie on the universal curve of Fig. 7(b). The pdf's of the first two have no transformation under which (5) holds. Symmetry is nevertheless established. This confirms that skewness is primarily a property of large-scale structures.⁹ Both w_{xx} and w_{zz} (by continuity) are restricted to be zero at the boundary, whereas w_{xz} is the vertical derivative of the universal function w_x . Therefore all three pdf's show universality and to excellent approximation fall on the same curve, Fig. 7(b). In Fig. 8 we show pdf's for T'_{xx} and T'_{zz} . The pdf's for the last quantity do not have a symmetrizing transformation leading to (4). Nevertheless, except near the wall for $P(\hat{T}'_{zz})$ the pdf's are symmetric and exhibit a tendency toward universality. This is even more true for T'_{xz} which also does not have a symmetrizing transformation but has pdf's very well fit by Fig. 8(a).

Thus we conclude that whatever the mechanism forcing universality, as might be expected, it is more effective on higher derivatives.

V. OTHER MEAN QUANTITIES

Figure 9 contains plots of T'_{rms} , u'_{rms} , w'_{rms} , as well as $\langle wT' \rangle$ (and its covariance) and $(d/dz)\langle T' \rangle$. In certain instances for a range of z , the curves are well fit by power laws and this has been indicated. Arguments leading to power-law dependence are similar to those leading to the inertial sublayer (log layer) for turbulent wall-bounded flows.²⁴ In brief, once away from the diffusive layers adjacent to a wall the only available length scale is the distance to the boundary. Prandtl²⁵ applied this to the convection problem and one finds^{24,26}

$$T'_{rms} \propto z^{-1/3}, \quad w'_{rms} \propto z^{1/3}, \quad \frac{d\overline{T'}}{dz} \propto z^{-4/3} \quad (8)$$

in this region, where T'_{rms} and w'_{rms} are the rms temperature and vertical velocity fluctuations (Kraichnan,²⁷ also using mixing length theory, has considered in detail the case in which the Pr number is allowed a wide range of values). A simple argument that leads to (8) is that since in the inviscid region the convective heat transport

$$\overline{wT'} = H_0 \quad (9)$$

is a constant, this implies that w and T' scale reciprocally with z . Thus, in the vertical momentum equation the lead

terms are

$$w \frac{\partial w}{\partial z} \propto T', \quad (10)$$

from which the scaling in (8) follows.

While T'_{rms} does show a sensible range for a $(-\frac{1}{3})$ power, the same is not true for w_{rms} . Though the convective heat transport $\langle wT' \rangle$ and the covariance $(\langle wT' \rangle / w_{rms} T'_{rms})$ are constant across the layer ($0.20 < z < 0.80$) except near the boundary, w does not scale reciprocally since the region over which $T' \propto z^{1/3}$ ($0.05 < z < 0.2$) falls closer to the boundaries. We also note that dT'/dz does not follow a $-\frac{4}{3}$ power. Townsend²⁸ and Thomas and Townsend²⁹ observed a -2 power, indicated as a dashed line in Fig. 9, a value also given by Carroll³⁰ and in a computation by Eidson *et al.*³¹ This value was first proposed by Malkus³² from theoretical arguments. However, we point out that a $-\frac{3}{4}$ power, the continuous straight line of Fig. 9, is a better fit to the calculation.

The lack of a consistent universal scaling regime is reminiscent of the situation for boundary-layer flows, where an argument similar to that leading to (8) produces the *log layer* for the mean velocity.³³ However as has been known for some time, not all quantities follow the universal scaling. To account for the lack of universality Townsend³⁴ and later Bradshaw³⁵ postulated the notion of *active* and *inactive* portions of the flow. In their explanation they invoke the idea of large (integral scale) eddies entering the boundary regions at infrequent times and marring the universality of some quantities.

In the present case, the underlying scaling arguments assume a semi-infinite domain in the vertical direction without horizontal wind,²⁶ and so might be thought to be applicable outside the dissipative sublayer at a wall. Recent experiments by the Chicago group indicate a sustained symmetry breaking *wind*. Also for the numerical simulations already discussed,^{6,7} the roll motions act as a winds since their time scale is of relatively long duration although they have zero mean. In any event this more general case changes the above dimensional reasoning and is treated in Monin and Yaglom²⁴ who find general classes of possible functional dependences. We do not pursue this further since

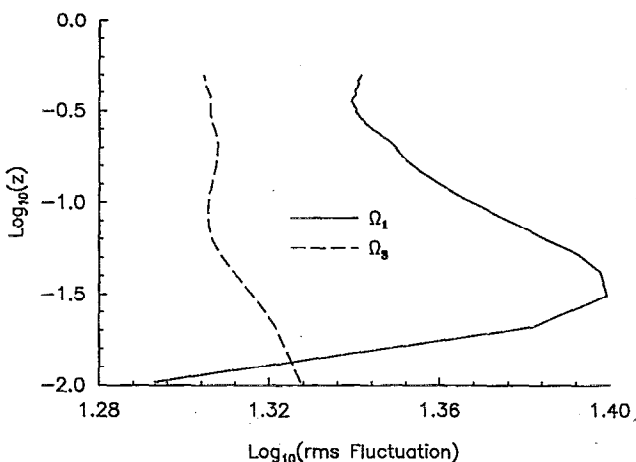


FIG. 10. Log-log plot of rms fluctuation vorticity components Ω_1 and Ω_3 .

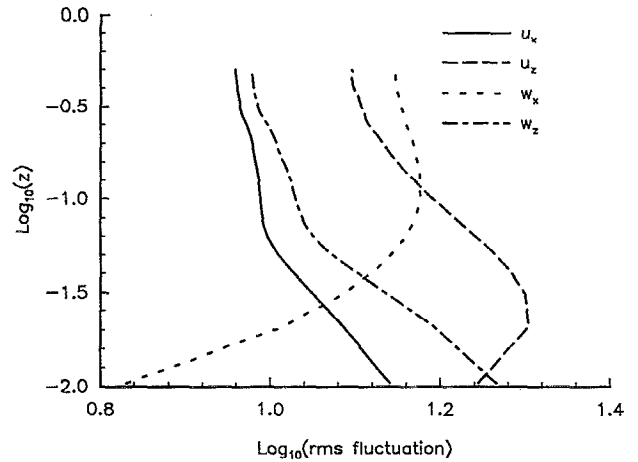


FIG. 11. Root mean square fluctuation in u_x , u_z , w_x , and w_z against vertical distance.

scaling does not appear to be a dominant effect.

Since all the pdf's considered are given in the normalization (3), it is of interest to present the remaining variances of the quantities considered with respect to their variation in the vertical direction z . The rms fluctuation of the two components of vorticity are plotted in Fig. 10. Figures 11–13 show the rms fluctuation for the first and second derivative quantities. Since pdf's of the raw variables follow from these plots this completes the single-point probabilistic description of all the relevant quantities.

While scaling does not appear to account for the universality another feature of the pdf's does help explain the collapse of pdf's onto universal curves. We observe that the above symmetric pdf's are well approximated by the family of curves

$$P(\alpha) = Ce^{-|\alpha|^{p/k}}, \quad (11)$$

where $C = C(p, k)$ is easily chosen so that there is unit area under the curve. $p = 2$ corresponds to a Gaussian distribution, $p = 1$ corresponds to an exponential distribution, and p less than one indicates a flatter *intermittent* distribution. All

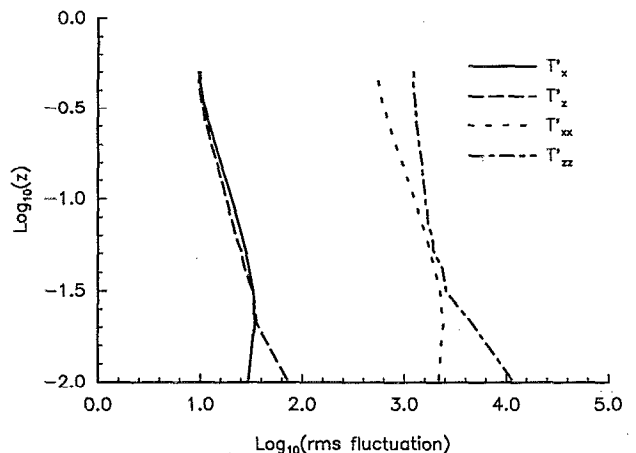


FIG. 12. Root mean square fluctuation in T'_x , T'_z , T'_{xx} , and T'_{zz} against vertical distance.

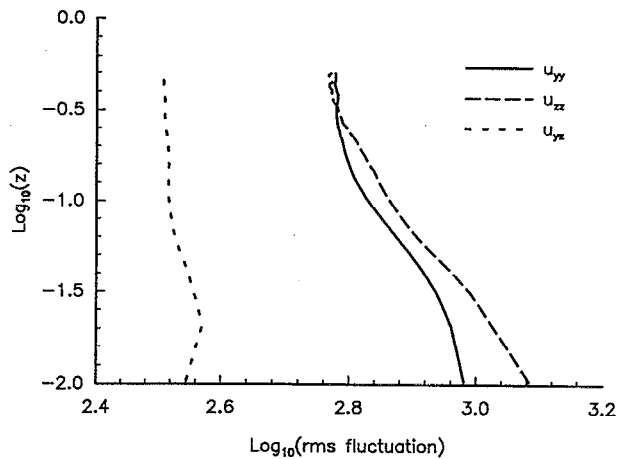


FIG. 13. Root mean square fluctuation in u_{yy} , u_{zz} , and u_{xz} against vertical distance.

the even moments of this distribution depend on p and k , while the odd moments are identically equal to zero. Closer to the boundaries the distributions are intermittent and the pdf's are flared out corresponding to p less than 1. As universality is approached the value of p decreases and in the universal regime since the level of intermittency can be expected to be uniform in the value of p ; i.e., it will be independent of the vertical location. Although k , which measures the width or the standard deviation of the pdf, can vary in the universal regime for the raw variables, once the raw variables are normalized by the rms fluctuation the value of k is dictated to be $[\Gamma(\frac{1}{2})/\Gamma(\frac{3}{2})]^{p/2}$ so that the normalized standard deviation is unity. Therefore in the universal regime p and k (which now depends only on p) are constants. Therefore as long as the level of intermittency (or p) reaches an asymptotic value, indicating universality, the collapse of the normalized pdf's can be explained. As already mentioned the approach to universality is rapid in the case of variables that are fixed at the boundaries.

VI. CONCLUDING REMARKS

An overall survey of the pdf's that have been exhibited leads one to believe that there is an active mechanism forcing the pdf's toward universal form. Both the degree to which this is true and the resulting shape of the pdf depend on the dominant relevant eddy size, i.e., on the number of derivatives being considered. In general the smaller the eddies, the more quickly is universality established, and the more intermittent (flared skirts) the shape of the pdf. As has been observed by She *et al.*⁹ skewness is essentially a large-scale property, while flatness is a small-scale effect.

As might be expected the presence of boundaries mars universality and wide departures from universal behavior can be expected in the neighborhood of a boundary. A boundary can act in two extremely different ways. It can pin down a fluctuation. For example, w , T' , w_x , u_z ,... are all restricted to vanish at a boundary. On the other hand Ω_3 , T'_z , w_z , u_y , u_x ,... are all unrestricted in that any fluctuation in those quantities is permitted at the boundary. Another important ingredient in determining the form of a pdf is sym-

metry. If a transformation of the form (4) is applicable then a symmetric pdf results. In certain instances this is only achieved at the midplane, e.g., w and T' . While in other cases symmetric pdf's must be obtained (assuming that there exists sufficient data) at all elevations, e.g., u , w_x , u_z ,...

As a general rule, at a boundary, and in its neighborhood, if there is no restriction imposed on the quantity, one should expect all manner of possible fluctuations to appear. This helps to explain why, for example, $P(\hat{\Omega}_3)$ has relatively wide skirts in the neighborhood of the boundary, and as a result shows a slower tendency to universality. By comparison u_z must be zero at a boundary and thus does not develop wide skirts in the neighborhood of a boundary. Unlike $P(\hat{\Omega}_3)$, $P(\hat{u}_z)$ tends very quickly to a universal form, Fig. 4.

The cases of $P(\hat{T}')$ and $P(\hat{w})$ are of interest to consider from the perspective of the present discussion. In both instances the quantity in question is forced to vanish at the boundary. This, however, has little effect in restricting the corresponding pdf. Although each must be symmetric in the midplane, this is not true elsewhere and the passage to the symmetric pdf is difficult to characterize.

The mechanism that is responsible for the tendency towards universality is not obvious. Kraichnan^{5,18} has produced a simple heuristic model of intermittency based on a closure approximation which exhibits independence of Reynolds number. This may be indicative of the processes at work and which bring about universality. Further investigation of this effect is clearly indicated.

While our deliberations are based on the computation of RB convection, at one value of Ra, it seems clear that they should be generalize to other flow geometries and other values of the control parameter. The approach to universality that we have followed in terms of the vertical distance from a wall is doubtless better expressed in terms of a wall normalized variable. For channel or boundary-layer flows this would be the usual wall normal coordinate, while in the present case z/δ is the suitable variable. When the pdf's are expressed in such terms we anticipate that universality will also hold with varying control parameters. A study of available channel flow data strongly indicates universal forms for the corresponding pdf's.

ACKNOWLEDGMENT

The authors are grateful to Bruce Knight for many helpful discussions.

The work reported here was supported by the Defense Advanced Research Projects Agency (University Research Initiative N00014-86-K0754) and by the National Aeronautics and Space Administration under Contract No. NAS1-18605 while one of us (L. S.) was in residence.

¹S. B. Pope, Prog. Ener. Combust. Sci. **11**, 119 (1985).

²Ja. G. Sinai and V. Yakhot, Phys. Rev. Lett. **63**, 1962 (1989).

³V. Yakhot, Phys. Rev. Lett. **63**, 1965 (1989).

⁴H. Chen, S. Chen, and R. Kraichnan, Phys. Rev. Lett. **63**, 2657 (1989).

⁵R. H. Kraichnan, Phys. Rev. Lett. **65**, 575 (1990).

- ⁶L. Sirovich, S. Balachander, and M. R. Maxey, *Phys. Fluids A* **1**, 1911 (1989).
- ⁷S. Balachandar, M. R. Maxey, and L. Sirovich, *J. Sci. Comput.* **4**, 219 (1989).
- ⁸R. M. Kerr, *J. Fluid Mech.* **153**, 31 (1985).
- ⁹Z.-S. She, E. Jackson, and S. A. Orszag, *J. Sci. Comput.* **3**, 407 (1988).
- ¹⁰F. Heslot, B. Castaing, and A. Libchaber, *Phys. Rev. A* **36**, 5870 (1987).
- ¹¹B. Castaing, G. Gunaratine, F. Heslot, L. Kadanoff, A. Libchaber, S. Thomas, X. Z. Wu, S. Zaleski, and G. Zannetti, *J. Fluid Mech.* **204**, 1 (1989).
- ¹²M. Sano, X. Z. Wu, and A. Libchaber, *Phys. Rev. A* **40**, 6421 (1989).
- ¹³K. R. Sreenivasan, R. Narashima, and A. Prabhu, *J. Fluid Mech.* **137**, 251 (1983).
- ¹⁴F. N. Frenkiel, P. S. Klebinoff, and T. T. Huang, *Phys. Fluids* **22**, 1606 (1979).
- ¹⁵F. Anselmet, Y. Gagne, E. J. Hopfinger, and R. A. Antonia, *J. Fluid Mech.* **140**, 63 (1984).
- ¹⁶V. Yakhot, S. A. Orszag, S. Balachandar, E. Jackson, Z.-S. She, and L. Sirovich, in *Proceedings of the 6th Beersheba Seminar*, Jerusalem, edited by H. Branover (AIAA, Washington, DC, 1990).
- ¹⁷R. Kraichnan in *New Perspectives in Turbulence*, edited by L. Sirovich (Springer-Verlag, Berlin, 1990).
- ¹⁸R. Kraichnan, in Ref. 16.
- ¹⁹P. G. Drazin and W. H. Reid, *Hydrodynamic Stability* (Cambridge U. P., Cambridge, 1981).
- ²⁰L. Sirovich, *Q. Appl. Math.* **45**, 572 (1987).
- ²¹A. N. Kolmogorov, *C. R. Acad. Sci. (USSR)* **30**, 301 (1941).
- ²²C. Foias, O. Manley, and L. Sirovich, *Phys. Fluids A* **2**, 464 (1990).
- ²³R. Kraichnan, *Phys. Fluids* **10**, 2080 (1967).
- ²⁴A. S. Monin and A. M. Yaglom, *Statistical Fluid Mechanics* (MIT Press, Cambridge, 1975), Vol. 2.
- ²⁵L. Prandtl, *Beitr. Phys. Atmos.* **19**, 188 (1932).
- ²⁶C. H. B. Priestly, *Aust. J. Phys.* **7**, 176 (1954).
- ²⁷R. Kraichnan, *Phys. Fluids* **5**, 1374 (1962).
- ²⁸A. A. Townsend, *J. Fluid Mech.* **5**, 209 (1959).
- ²⁹D. B. Thomas and A. A. Townsend, *J. Fluid Mech.* **2**, 473 (1957).
- ³⁰J. J. Carroll, *J. Atmos. Sci.* **33**, 642 (1976).
- ³¹T. M. Eidson, M. Y. Hussaini, and T. A. Zang, in *Notes on Numerical Fluid Mechanics* (Vieweg, Braunschweig, 1986), Vol. 15, p. 188.
- ³²W. V. R. Malkus, *Proc. R. Soc. London Ser. A* **225**, 196 (1954).
- ³³H. Tennekes and J. Lumley, *A First Course in Turbulence* (MIT Press, Cambridge, MA 1972).
- ³⁴A. A. Townsend, *J. Fluid Mech.* **11**, 97 (1961).
- ³⁵J. Bradshaw, *J. Fluid Mech* **30**, 241 (1967).